Spring 2017

Improving Energy Efficiency for IoT Communications in 5G Networks

Gary Su
San Jose State University

Improving Energy Efficiency for IoT Communications in 5G Networks

A Writing Project Report

Presented to

The Faculty of the Department of Computer Science

San Jose State University

In Partial Fulfillment

Of the Requirements for the Degree

Master of Science

By

Gary Su

May 2017

ABSTRACT

Increase in number of Internet of Things (IoT) devices is quickly changing how mobile networks are being used by shifting more usage to uplink transmissions rather than downlink transmissions. Currently, mobile network uplinks utilize Single Carrier Frequency Division Multiple Access (SC-FDMA) schemes due to the low Peak to Average Power Ratio (PAPR) when compared to Orthogonal Frequency Division Multiple Access (OFDMA). In an IoT perspective, power ratios are highly important in effective battery usage since devices are typically resource-constrained. Fifth Generation (5G) mobile networks are believed to be the future standard network that will handle the influx of IoT device uplinks while preserving the quality of service (QoS) that current Long Term Evolution Advanced (LTE-A) networks provide. In this paper, the Enhanced OEA algorithm was proposed and simulations showed a reduction in the device energy consumption and an increase in the power efficiency of uplink transmissions while preserving the QoS rate provided with SC-FDMA in 5G networks. Furthermore, the computational complexity was reduced through insertion of a sorting step prior to resource allocation.

ACKNOWLEDGEMENTS

I would like to sincerely thank Dr. Melody Moh for providing guidance and giving me helpful advice that I will carry with me in my life. Her encouragement has helped me successfully complete this project. I would also like to thank my committee member Dr. Sunuey Kim for her continuous support and giving me her valuable time. Additionally, I would like to thank Dr. Thomas Austin for being my committee member and giving his time to help me with this project. Finally, I am thankful to have my family and friends support my endeavors.

TABLE OF CONTENTS

List of Acronyms

3GPP	3rd Generation Partnership Project
eNodeB	E-UTRA Node B
FFT	Fast Fourier Transform
IFFT	Inverse Fast Fourier Transform
IoT	Internet of Things
LTE	Long Term Evolution
LTE-A	Long Term Evolution Advanced
MCS	Modulation and Coding Scheme
OFDMA	Orthogonal Frequency Division Multiple Access
PAPR	Peak-to-Average Power Ratio
PSK	Phase Shift Keying
QAM	Quadrature Amplitude Modulation
QoS	Quality of Service
RB	Resource Block
RE	Resource Element
SC-FDMA	Single Carrier Frequency Division Multiple Access
SNR	Signal to Noise Ratio

I. Introduction

Internet of Things (IoT) devices are increasingly entering today's market. Similar to smart phones, many IoT devices rely upon a wireless Ethernet connection to utilize data services. These IoT devices often have a characteristic of large volumes at unknown locations and thus using a wired connection would not be practical. Long Term Evolution Advanced (LTE-A) is the current 4th generation (4G) mobile communication standard. It is commonly used by smartphones as the data service medium to connect with the internet. Though LTE was created to provide internet access via wireless connection, it would not be able to handle the volume of IoT devices that is projected to need data services [1]. Consequently, the fifth generation (5G) mobile network will be the solution used to provide a data connection for these IoT devices. As a result, 5G is the next evolution of mobile communication standards that is projected to have higher speeds, larger bandwidth capacity, better coverage, and improved reliability to better handle the influx of data demands from IoT devices [2]. These IoT devices differ from smartphones as they will shift more usage to the uplink transmission rather than downlink services.

LTE-A and 5G uplink transmission have a number of constraints. One of these constraints is power consumption. With downlink transmission, the power required to transmit signal is consumed at the E-UTRAN Node B (eNodeB), which typically does not rely upon a limited power source such as a battery. Smartphones or IoT devices rely on using a battery as a power source. Unfortunately, devices performing wireless uplink transmission in the LTE-A and 5G networks can consume a large amount of power. In uplink transmission, resources such as computational hardware, wireless antennas, and power source are constrained and limited [3]. This is why the multiple access scheme between downlink and uplink transmission differ for both LTE-A and 5G networks. Downlink transmission in these networks uses Orthogonal Frequency Division Multiplexing Access (OFDMA) while uplink transmission uses Single Carrier Frequency Division Multiplexing Access (SC-FDMA). Both downlink and uplink transmission require radio resources to be allocated. For the purposes of this research paper, resource allocation is done only for uplink transmission.

An essential component in wireless communication is having an adequate signal-to-noise (SNR) ratio. The transmitted signal can be increased or decreased depending on the power that the device uses for transmission [3]. The noise is typically the combination of many factors, some of which can be path loss, shadowing, and interference. For resource allocation, the resource is considered the frequency in which the signal should be transmitted. Higher frequencies are more sensitive to the environment as they are

affected more by other wireless signals and noise. Path loss depends on the distance between the IoT device's and the eNodeB, transmitting and receiving antenna gain, and the transmitted frequency [4]. Since the SNR can differ between each resource channel and connected device, the radio resource allocation algorithm is important since it distributes the resources and this in turn affects the behavior of the device's power control due to the varying SNR.

II. Problem Description

IoT devices are resource constrained and having to recharge or replace the batteries in these devices would become problematic. With power control, the eNodeB provides a feedback signal in which the connected device can utilize to determine the amount of output power that it needs to maintain a communicable channel [5]. Thus, radio resource allocation algorithms will need to more efficiently consume IoT device power through smart and selective resource allocations.

This paper is organized as follows. Section II provides background information for LTE-A and 5G uplink transmission and resource allocation. In Section III, related works are discussed. In Section IV, the system model is explained along with the resource allocation algorithms used in this paper including the proposed modified algorithm. The experiment and simulation results are presented in Section IV, which will be followed by the conclusion in section V.

III. Background

A. Power Control

One of the ways to influence a device's power consumption is to perform power control [4]. Here, the eNodeB provides a signal feedback that the IoT device would use to adjust its power output for the transmitted signal [5]. In this research paper, the signal feedback comes in the form of a metric containing a set of SNR calculations where the signal is the transmission power and the noise is a combination of thermal noise, path loss, and shadowing. The transmission power is assumed to initially be at the maximum allowed power but is adjusted with power control after resource allocation.

B. LTE-A and 5G Resources

LTE-A resources come in the form of frequency bandwidths that are allocated to users. More specifically, they are referred to as resource blocks (RBs). A resource block (RB) can be defined by the sum of resource elements (RE). REs are defined as one subcarrier with a duration of one LTE Symbol. A RB in the LTE-A system is shown in Figure 1.

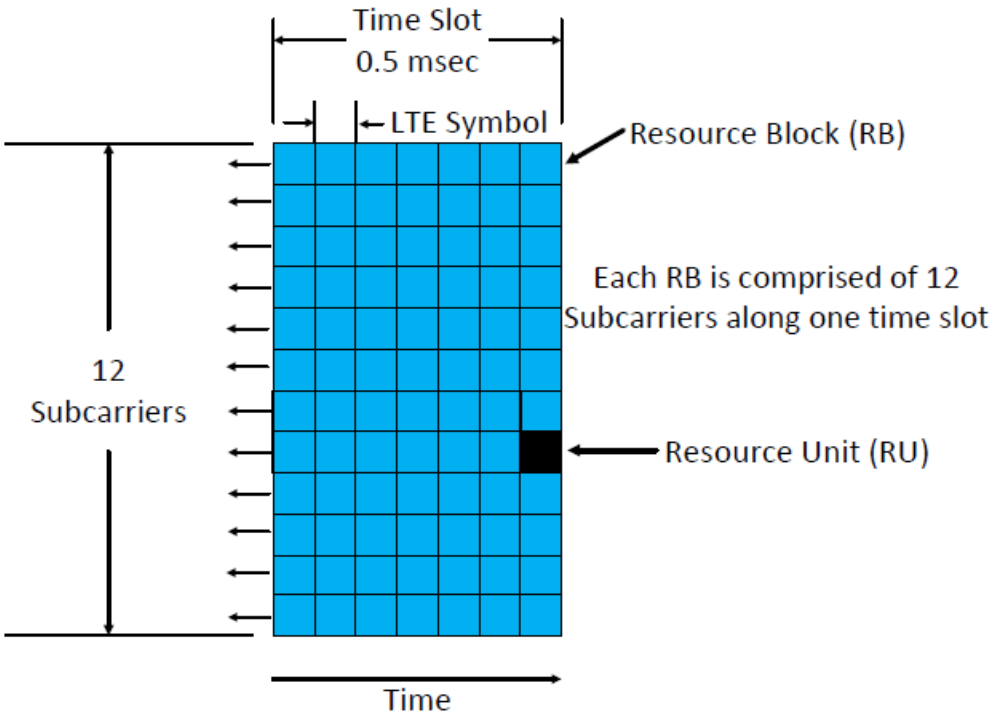

Figure 1. Resource block in the LTE-A and 5G system [6]

In LTE-A and 5G systems, a RB consists of 12 subcarriers over one time slot of 0.5 milliseconds [6]. A sub-frame contains two time slots. The number of LTE symbols per RB typically depends on the length of the cyclic prefix. The cyclic prefix is the added symbol repetition that serves as a guard interval and allows for easier frequency domain processing. With a normal cyclic prefix, there will 7 LTE symbols per RB. An extended cyclic prefix will result in 6 LTE symbols per RB.

For a given transmission bandwidth, the 3rd Generation Partnership Project (3GPP) set the standard for the number of resource blocks available. More specifically, Table I below describes the number of resource blocks for given transmission bandwidths [7].

Table I. LTE-A RB SPECIFICATION FOR TRANSMISSION BANDWIDTHS

Transmission Bandwidth	1.4 MHz	3 MHz	5 MHz	10 MHz	15 MHz	20 MHz
Number of Resource Blocks	6	15	25	50	75	100

Occupied Subcarriers	72	180	300	600	900	1200

i. Resource Allocation in LTE-A and 5G

Resource allocation in LTE-A networks is an essential interaction between the eNodeB and its connected IoT device. During resource allocation, RBs are distributed among users for a certain amount of time. This means that the eNodeB provides a transmission channel for the connected IoT device [8]. As previously mentioned, the transmission power of the IoT device depends on many factors when using power control. This is due to the factors contributing to the noise between the IoT device and the eNodeB.

ii. OFDMA and SC-FDMA

OFDMA is a multiple access scheme that ensures orthogonality between frequencies which ultimately gets rid of the intracellular interference. Inter-cell interference still remains though. In OFDMA, wireless channels are broken down into smaller bandwidths in order to reduce delay spreads. Each channel is a RB with a bandwidth of 180 kHz. Within the RB are 12 subcarriers with a subcarrier spacing of 15 kHz [9]. With OFDMA, resources can be scheduled via frequency and/or time [10].

SC-FDMA is a special case of OFDMA. With SC-FDMA, an extra FFT step is performed on the transmitter side to convert signal to time domain before subcarrier mapping occurs; consequently, an extra IFFT step must also be performed on the receiver side [11]. The extra FFT step ensures that signals are transmitted only over a time domain with no choice of using the frequency domain like in OFDMA. This can be seen in the Figure 2. Because of this, SC-FDMA has a lower peak-to-average-power ratio (PAPR) which makes it a more ideal uplink transmission scheme over OFDMA [1] [12] [13]. This is because mobile devices have a limited source of power as they rely upon a battery source. Figure 3 below describes the flow of steps required in SC-FDMA.

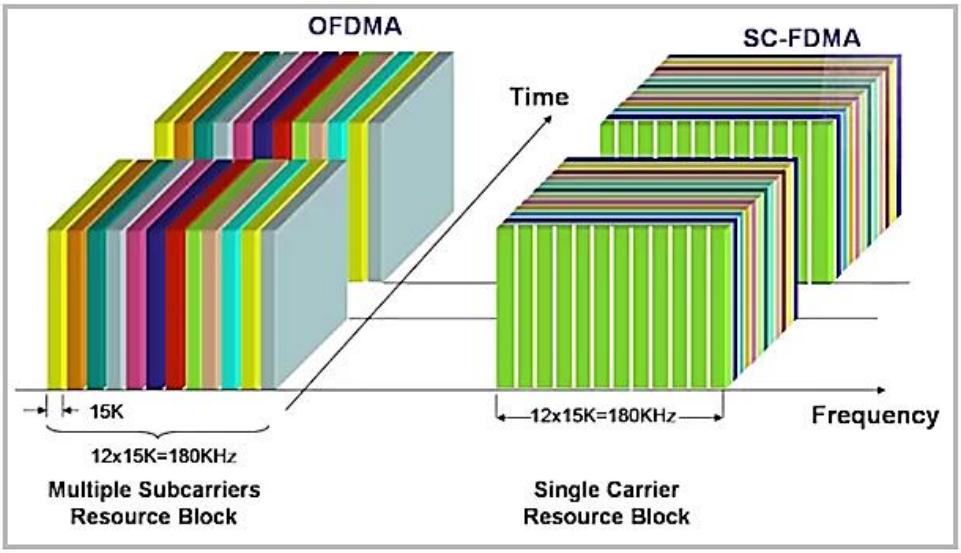

Figure 2. Data Transmission of OFDMA and SC-FDMA [14]

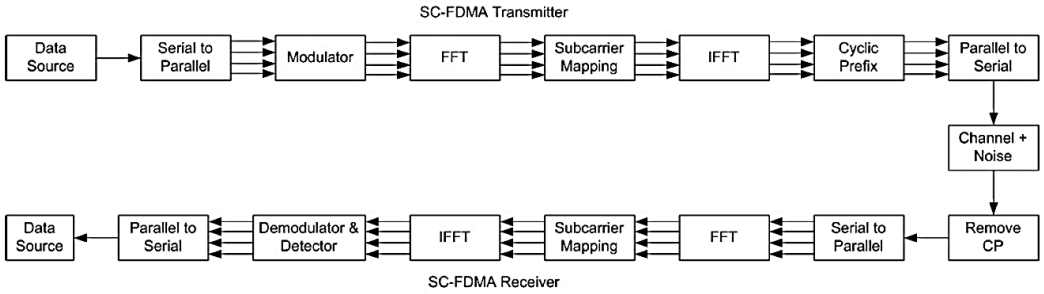

Figure 3. Diagram of SC-FDMA System [10]

iii. Modulation and Coding Schemes for LTE-A

With the OFDMA and SC-FDMA techniques, there are a number of modulation and coding schemes (MCS), which dictate how data bits are encoded onto wireless signal after the signal has gone through a discrete Fourier Transform. Currently there are two types of MCS which include phase shift keying (PSK) and quadrature amplitude modulation (QAM) [15]. Resources are radio signal. While encoding these radio signal with data bits, it is possible to shift the phase of the signal or modify its amplitude. Doing so helps to distinguish these data bits on the receiving end, where a FFT or IFFT would attempt to recover the original signal. Table II is a combination of two tables that shows the bits per symbol and minimum required SNR that is associated with different MCS [15] [16]. Since uplink transmission is resource constrained, dynamic MCS cannot be done unless the device has all the necessary antennas. As a result, this research paper utilizes only 16-QAM as the MCS. An example of 16-QAM constellation diagram is shown below in Table II.

Table II: MODULATION SCHEMES

Modulation	Bits per Symbol	Minimum SNR Required
BPSK	1	3.5
QPSK	2	5.5
8PSK	3	--
16QAM	4	12
32QAM	5	--
64QAM	6	20

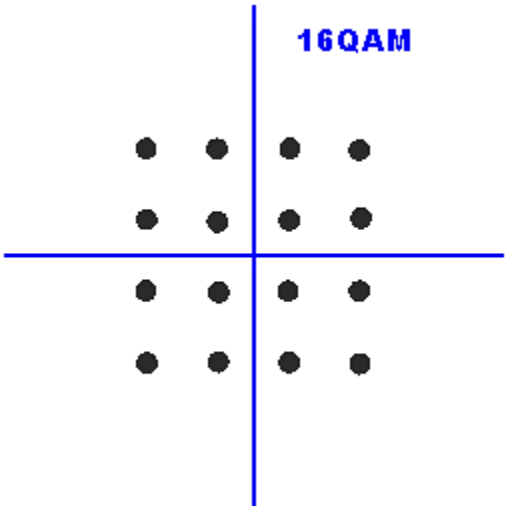

Figure 4: Example of 16-QAM Constellation Diagram [8]

iv. Constraints with SC-FDMA

SC-FDMA was selected as the uplink transmission for LTE systems due to its low PAPR. To maintain this low PAPR, however, there are constraints that must be followed [6] [17]. First, each whole RB must be allocated to just one device. In OFDMA, one RB can be shared among multiple devices, giving much more diversity and flexibility with resource allocation. Secondly, all RBs allocated to the same device must be adjacent.

IV. Related Works

Many papers have addressed power consumption in LTE uplink transmission but generally view the LTE uplink resource allocation as an optimization problem. One approach was to evaluate the spectral

efficiency and peak data rate of a distributed resource management [1]. The resource allocation problem has also been viewed as an optimization problem and solved through applying set partitioning [8]. This algorithm added computational complexity to increase the spectral efficiency. Other works approached the resource allocation problem with a deeper mathematical perspective [6][18][19]. When the problem is viewed as a dual optimization problem where the throughput needs to be maximized while minimizing energy consumption, the Lagrange equation can be used to solve the problem [6]. Another approach for solving the dual optimization is to use the Canonical Duality Theory and setting up the problem in the form of a quadratic equation [18]. Another paper proposes the OEA radio resource allocation algorithm in order to minimize energy consumption through using a metric and applying a greedy search for determining the order of resource allocation [17]. Finally, an exhaustive search can be used to identify the optimal resource allocation in terms of throughput [20].

V. System Model and Resource Allocation Algorithms

A. System Model

i.RB Channel Capacity

Although each RB has a bandwidth of 180 kHz, the channel capacity depends on the SNR. More specifically, the Shannon—Hartley formula is used to describe the RB capacity.

$$C = B \log_2 (1 + S/N)$$

ii.Throughput

In this paper, the throughput is defined as the data rate. Since SC-FDMA is used here, the data rate can be limited by the modulation scheme rather than the channel capacity. More specifically, an environment where the noise is much greater than the signal would limit the throughput due to having a low channel capacity. In this paper, the limitation of throughput comes from the modulation scheme that is used, which is 16-QAM. Thus, the throughput can be calculated in terms of the bits per resource element and the number of allocated RBs [22] [23]. This can be described as

$$T = N_{sc} * N_{us} * \beta * L / t$$

where

- N_{sc} is the number of subcarriers in one RB.
- N_{us} is the number of uplink LTE symbols in one RB.
- β is the bits per resource element which depends on the modulation.

- L is the number of allocated RB.
- t is the time slot which is 0.5 ms.

iii. Path Loss

For this paper, log-distance path loss was calculated using two formulas. Path loss is initially calculated using Friis free space model [24] which can be described as

$$PL_0 = P_r / P_t = (G_t G_r \lambda^2) / (4\pi d)^2$$

where

- P_r is the received power in Watts.
- P_t is the transmitted power in Watts.
- G_t is the gain of the transmitter antenna.
- G_r is the gain of the receiver antenna.
- $\lambda = 3 * 10^8 / f$, is the wavelength of the carrier calculated and f is the frequency of the carrier.
- *d* is the distance between transmitter and receiver.

Then, an extension of Friis free space model is applied to calculate the log-distance path loss which includes a shadowing effect. The log-distance path loss equation from [4] also converts to dB and can be described as

$$PL\ (dB) = 10 \log_{10} (PL_0) + 10n \log_{10}(d) + \chi$$

where

- χ is a zero-mean Gaussian distributed random variable with standard deviation σ [4].
- *n* is the path loss exponent set to 2.7.
- *d* is the distance between transmitter and receiver.

iv. Thermal Noise

The thermal noise is calculated using the equation from [25] that can be described as

$$N_{dBm} = -174 + 10 \log10 (\Delta f) \qquad (5)$$

where

- Δf is the bandwidth in Hz.

Since the eNodeB channel is 5 MHz, the thermal noise power is calculated to be -107 dBm and assumed to remain constant.

v.Power Control

The power control mechanism is borrowed from [17]. It readjusts the power of a IoT device depending on the number of allocated RBs and the ratio of the target SNR vs the calculated SNR taken from the matrix metric M_x. This is described as

$$P_{IoT} = P_{max} / L * \tau_s / \tau_A \quad (6)$$

where

- P_{max} is the maximum transmission power equal to 21 dBm
- L is the number of allocated RB
- τ_s is the target SNR equal to 12
- τ_A is the minimum SNR of all allocated RB from matrix metric M_x

B. Resource Allocation Algorithms

The proposed algorithm is a variation of the OEA algorithm that was previously proposed in another paper [17]. An overview of the three algorithms' steps are shown below.

Definitions:

- Let N_{IoT} be the total number of IoT devices.
- Let N_{RB} be the total number of RB.
- Let M_x be the N_{IoT} x N_{RB} matrix such that (for all) m_{ij} (element) M_x, $1 \leq i \leq N_{IoT}$, $1 \leq j \leq N_{RB}$, m_{ij} is the SNR for pairing of *i*th IoT device (IoT_i) & *j*th RB (RB_j).
- Let A_k be the N_{IoT} x 1 matrix that is the average SNR of each IoT device across all RBs in M_x.
- Let A_c be the 1 x N_{RB} matrix that is the average SNR of each RB across all IoT devices in M_x.

Round-Robin Resource Allocation Algorithm:

1. For each IoT device, IoT_k
    a. Find the first available RB_c
    b. Assign RB_c to IoT_k
    c. Expand resource allocation until QoS is met
        i. Find RB_d such that index d = c + 1 or d = c – 1
        ii. Assign RB_d to IoT_k

OEA Resource Allocation Algorithm [17]:

1. Initialize M_x of N_{IoT} x N_{RB} with initial SNR calculations
2. Sort m_{ij} (epsilon) M_x

3. Repeat the following until all devices served or no more RB available:
    a. Find $m_{k,c} = max_{ij} \{ M_x \}$, $1 <= i <= N_{IoT}$, $1 <= j < N_{RB}$ such that the pairing of IoT_k with RB_c gives max SNR
    b. Assign RB_c to IoT_k
    c. Update device power allocation using Eqn. (6)
    d. Expand resource allocation until QoS is met
    e. Find $m_{k,d} = max_{ij} \{ M_x \}$ such that index d = c + 1 or d = c – 1
    f. Assign RB_d to IoT_k

Enhanced OEA Resource Allocation Algorithm:

1. Initialize Mx of NIoT x Nrb with initial SNR calculations
2. Initialize average SNR of device and RB into Ak and Ac, respectively
3. Sort Ak and Ac
4. Repeat the following until all devices served or no more RB available:
    a. Find ak = maxi { Ak } and ac = maxj { Ac } such that the pairing of IoTk with RBc gives two max averages of SNR from Ak and Ac
    b. Assign RBc to device k
    c. Update device power allocation using Eqn. (6)
    d. Expand resource allocation until QoS is met
        i. Find ad = maxj { Ac } such that index d = c + 1 or d = c – 1
        ii. Assign RBd to IoTk

One of the primary differences between the Enhanced OEA algorithm and the OEA algorithm is the metric that is used. The OEA algorithm uses a greedy algorithm that consistently prioritizes the highest metric in M_x, which is a matrix of N_{IoT} x N_{RB}. The Enhanced OEA algorithm, however, further processes M_x into two matrices A_k of size N_{IoT} x 1 and A_c of size 1 x N_{RB}, which are used to determine resource allocation. A_k is the average SNR of devices across all RBs. A_c is the average SNR of RBs across all devices. Aside from this difference, the resource allocation expansion is the same in all three algorithms. During this phase, the RBs adjacent to the initially allocated RBs are considered for allocation until the quality of service (QoS) is met. The QoS has been set to 1 Mbps following the LTE Category 0 performance requirement found in Table III below [21].

Table III. PERFORMANCE SUMMARY FOR IoT DEVICES

LTE CATEGORY 0 PERFORMANCE SUMMARY	
PARAMETER	LTE CAT 0 PERFORMANCE
Peak downlink rate	1 Mbps
Peak uplink rate	1 Mbps
Max number of downlink spatial layers	1
Number of UE RF chains	1
Duplex mode	Half duplex
UE receive bandwidth	20 MHz
Maximum UE transmit power	23 dBm

C. Complexity Analysis

The computational complexity was analyzed and is shown in Table IV below.

Table IV. COMPUTATIONAL COMPLEXITY OF RESOURCE ALLOCATION SCHEME

Algorithm	Computational complexity
OEA [17]	$O(N_{RB}N_{IoT} \log (N_{RB}N_{IoT}))$
Enhanced OEA	$O(N_{RB}N_{IoT})$

Sorting is an important step in reducing the complexity of the resource allocation algorithm. In the OEA algorithm, the step 1 is to initialize the metric matrix M_x which has a complexity of $O(N_{RB} * N_{IoT})$ since the SNR must be computed for all RB that can be allocated to each IoT device. Then step 2 sorts matrix M_x to help reduce the complexity during resource allocation. This results in a complexity of $O(N_{RB}*N_{IoT} \log (N_{RB}*N_{IoT}))$. Without the sorting from step 2, the complexity of OEA's step 3 would become $O(N_{IoT}^2) + O(N_{IoT}N_{RB})$ since M_x would need to be searched for each allocation. Finally in step 3, each IoT device gets assigned RBs which ultimately has a complexity of $O(N_{IoT})$. Resource allocation expansion has a constant complexity since only adjacent resources can be considered. The Enhanced OEA algorithm has the same steps as the OEA algorithm except that it introduces step 2 which computes average SNR across all RB and across all IoT devices, hence this modified algorithm has an added step with complexity of $O(N_{RB} * N_{IoT})$. However, the sorting complexity is reduced since the metric matrix M_x is processed into two matrices of smaller size. Because of this, the overall computational complexity for the sorting done in step 3 of the Enhanced OEA algorithm is $O(N_{RB}N_{IoT})$. To be more accurate, the Enhanced OEA complexity is $O(N_{RB}N_{IoT}) + O(N_{IoT} \log N_{IoT}) + O(N_{RB} \log N_{RB})$ but we assume the first term is bigger than other two since we do not know how many RB or IoT devices there are. Without the sorting done in step 3, the overall complexity of

Enhanced OEA's step 4 would become $O(N_{IoT}^2 * N_{RB})$. With sorting, step 4 of this algorithm has the same complexity of the OEA algorithm's step 3 which is $O(N_{IoT})$.

Further processing the SNR metric by taking the averages helps to ensure a more consistent quality of allocation for all IoT devices that need to be served. As the number of IoT devices increases, it is important to ensure a consistent quality of RB allocation. Using a greedy allocation, however, will cause the RB and IoT devices with lower SNR to remain towards the end of the resource allocation cycle. Thus processing the average SNR for IoT devices and RBs will help to balance the allocation cycle as there are more IoT devices.

VI. Experiments and Results

A. Simulation Inputs

First, a set of input files needed to be created that would represent the map and physical locations of the IoT devices relative to the eNodeB. Each input file consists of 1 eNodeB with a certain number of IoT devices. In this paper, the IoT devices are assumed to be stationary. It should be noted that the eNodeB is always at a fixed coordinate position in all input files. The IoT devices are randomly generated within 500 meters of the eNodeB's x coordinate position as well as the y coordinate position. An example of an input file with 12 IoT devices is shown in Figure 5.

UE	189	343	4
UE	635	150	4
UE	742	914	4
UE	976	619	4
UE	416	480	4
UE	649	109	4
UE	144	650	4
UE	616	954	4
UE	785	192	4
UE	956	90	4
UE	558	108	4
UE	294	756	4
eNB	500	500	4

Figure 5. Example of Input File Data

UE, abbreviated for User Equipment, signifies that it is an IoT device. The next number after that is the x coordinate and following is the y coordinate of the system. The last number in the row is the bits per symbol that it can support. This means that it will use 16-QAM modulation since that is the modulation corresponding to 4 bits per symbol. The x and y coordinates are generated using a random number

generator. As a result, 12 input files were created with the spectrum of having 1 IoT device to 12 IoT devices. Additionally, 10 sets of these 12 input files were created so that there could be an average calculation over each iteration of device number.

The following input parameters have been taken from [17]. First, the gain of the transmission antenna of the IoT device is 1 dBi. Second, the gain of the eNodeB antenna is 17 dBi. Third, the maximum device power is assumed to be 21 dBm, which translates to 125 mW. Fourth, the carrier frequency of 2.6 GHz. Fifth, the system bandwidth of 5 MHz. Sixth, log-normal shadowing sigma is 6 dB. The list of simulation inputs taken from [17] can also be seen in the full list of simulation parameters given in Table V below.

Table V: SIMULATION PARAMETERS

Carrier frequency	2.6 GHz
System bandwidth	5 MHz
Subcarrier spacing	15 kHz
Time slot duration	0.5 ms
eNodeB height	40 m
IoT antenna height	1.5 m
eNodeB antenna gain	17 dBi
IoT maximum transmission power	21 dBm (or 125 mW)
IoT antenna gain	1 dBi
IoT target throughput for QoS	1 Mbps
Log-normal shadowing	σ = 6 dB
MCS setting	16-QAM

When running the simulation, the input files are parsed and the result is used as parameters for calculating the path loss. Then parameters such as the carrier frequency, total number of IoT devices, total number of RB, number of LTE symbols, number of subcarriers, QoS requirement, maximum device transmission power, and the modulation scheme are passed into each resource allocation algorithm. Each respective resource allocation algorithm then allocates available RBs to the IoT devices requiring data services. Once all IoT devices have been served or there are no more available RBs, then the algorithms stop and perform power control for each UE.

The experiment data consisted of 10 sets of 12 input files. Each input file contained a set number of IoT devices. For example, there would be 10 sets of input files that have 1 IoT device, but also 10 sets of input files that have 2 IoT devices, and so on. Within each set, the x and y coordinate placement of the

IoT device was generated randomly so the main difference between input files was the location of the device relative to the eNodeB and the number of IoT devices. In all input files, the eNodeB is in a fixed position. The simulation only runs for one frame of RB allocation. Thus, it does not perform continuous allocation over time. Continuous allocation over time would refer to data transmission completing, and then releasing the RB for allocation to another IoT device. An overview of the simulation flow can be found below.

Overview flow of the simulation:

1. Provide the set of input data and other information
2. Parse and read the input data
3. Compute the metrics using all the input data and store into matrix M_x
    a. Compute the path loss with log normal shadowing
    b. Thermal noise is assumed to be constant
    c. Compute the channel gain
    d. Compute the SNR
4. Pass the matrix M_x to each resource allocation algorithm
5. Run the resource allocation algorithm with the metric and given input
6. Accumulate and compile the data collection statistics

B. Results

The OEA algorithm was analyzed and then a modification of this algorithm was proposed as the Enhanced OEA [17]. Both the Enhanced OEA algorithm and OEA algorithm utilize a SNR metric that is created from a series of calculations. The Round-robin algorithm does not use any metric to determine the resource allocation order. Rather, it performs resource allocation on a first-come first-serve basis. OEA algorithm uses the individual max SNR found in M_x while the Enhanced OEA algorithm uses the highest average SNR from matrices A_k and A_c computed from M_x.

When running the 3 algorithms provided with the same sets of input files, there were a number of interesting results. The proposed algorithm resulted in the same throughput, higher power efficiency, lower power consumption, and better utilization of RB channels than the OEA algorithm. This was achievable because the RB channel capacity, which depends on the SNR, is not the true throughput for SC-FDMA. Rather, it is the maximum achievable rate via that channel. Instead, the throughput is limited by the MCS, which in this case is 16-QAM. The amount of data that can be encoded onto one RB channel depends on the MCS and the number of allocated RBs. The throughput is calculated using equation (2).

The throughput is obtained by multiplying the number of LTE symbols with the number of subcarriers times the bits per symbol and divides all this by the timeslot. Since the MCS is 16-QAM, a lower SNR is required and not all of the RB channel is completely used. If the MCS were 64-QAM, then there would be a greater possibility that all, if not more, of the RB channel would be utilized. However, higher modulations mean greater power consumption due to a greater requirement for SNR. Lower modulation schemes would result in lower spectrum efficiency. Thus 16-QAM was chosen as the MCS.

i.Throughput

For each input, the throughput was added to a running total that is outputted once the simulation finishes running all inputs. The results are shown in Figure 6 and Table VI below. The proposed algorithm has a similar throughput compared to OEA algorithm. The Round-Robin algorithm is consistently lower than both of the algorithms that use a metric to determine the resource allocation.

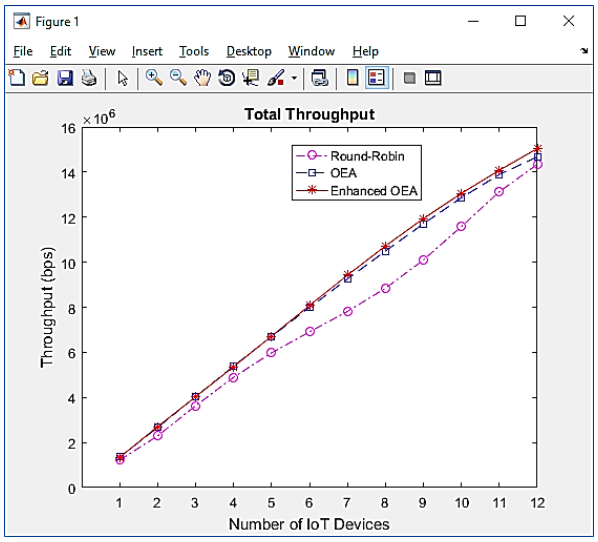

Figure 6. Total Throughput

Table VI: VALUES FOR TOTAL THROUGHPUT

# of Devices	Round Robin 1.0e+07 *	OEA 1.0e+07 *	Enhanced OEA 1.0e+07 *
1	0.1219	0.1353	0.1339
2	0.2291	0.2668	0.2702
3	0.3627	0.4031	0.4029
4	0.4894	0.5384	0.5362
5	0.5977	0.6705	0.6716
6	0.6909	0.7992	0.8078
7	0.7816	0.9251	0.9423
8	0.8843	1.0491	1.0719

9	1.0097	1.1704	1.1935
10	1.1580	1.2859	1.3054
11	1.3127	1.3888	1.408
12	1.4340	1.4674	1.5044

The Round-Robin algorithm is consistently lower than both of the algorithms that use a metric to determine the resource allocation.

ii.Resource Block Capacity

The next data result to monitor was the RB capacity when it gets allocated to an IoT device. This depends on the SNR that is calculated between the RBs and IoT device. The OEA and proposed algorithms both utilize the SNR metric that is defined as matrix M_x. The Round-Robin algorithm does not use the metric and thus consistently has a total RB capacity lower than both the OEA and proposed algorithms. The OEA algorithm has the highest RB capacity since it always assigns the RB to the IoT device with the highest calculated SNR. The proposed algorithm assigns according to the highest average SNR across both the RBs and IoT devices, meaning that the proposed algorithm's total RB capacity would be less than algorithm in [17]. This can be observed in Figure 7 and Table VII.

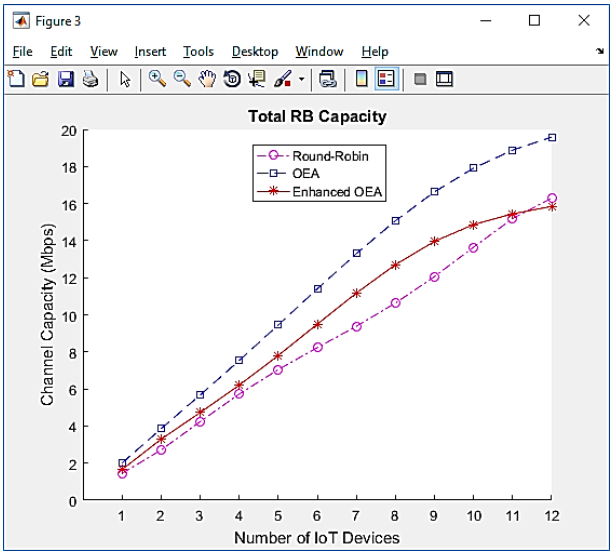

Figure 7: Total RB Capacity

Table II: VALUES FOR TOTAL RB CAPACITY

# of Devices	Round Robin	OEA	Enhanced OEA
1	1.4406	1.9965	1.6497
2	2.7032	3.8553	3.2864
3	4.2371	5.6704	4.7243

4	5.7224	7.5297	6.2021
5	7.0435	9.4502	7.8027
6	8.2273	11.3965	9.4948
7	9.3813	13.2988	11.174
8	10.6313	15.071	12.7045
9	12.0598	16.6292	13.9608
10	13.6438	17.9092	14.8684
11	15.1929	18.8854	15.446
12	16.2871	19.5883	15.8466

To further examine the RB capacity behavior, the maximum, minimum, and average RB capacities were plotted as shown in Figure 8a-e below. The values of the results can be found in Table VIII, Table IX, and Table X.

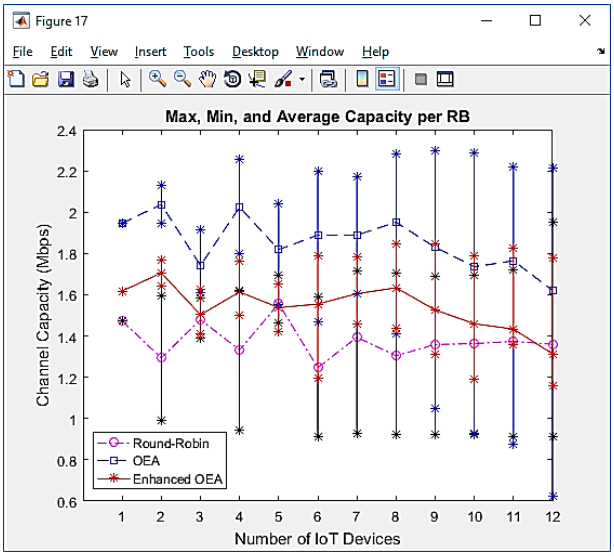

Figure 8a. Max, Min, and Average Capacity per RB

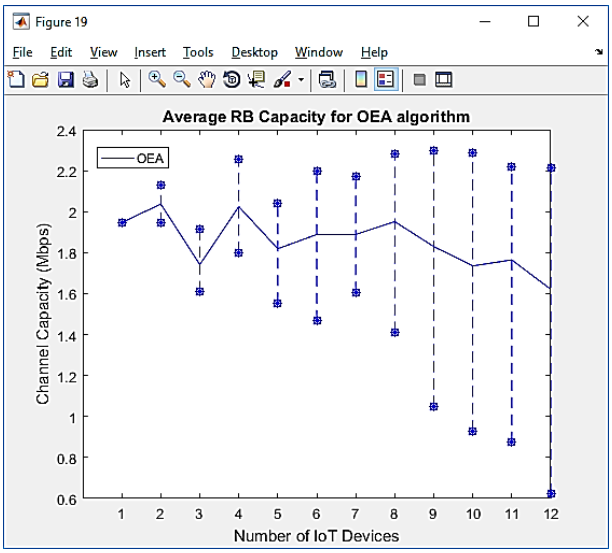

Figure 8b. Max, Min, and Average Capacity for OEA Algorithm

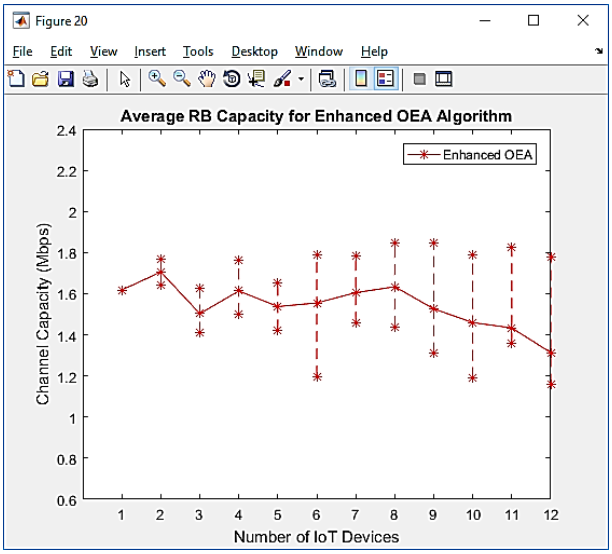

Figure 8c. Max, Min, and Average Capacity for Proposed Algorithm

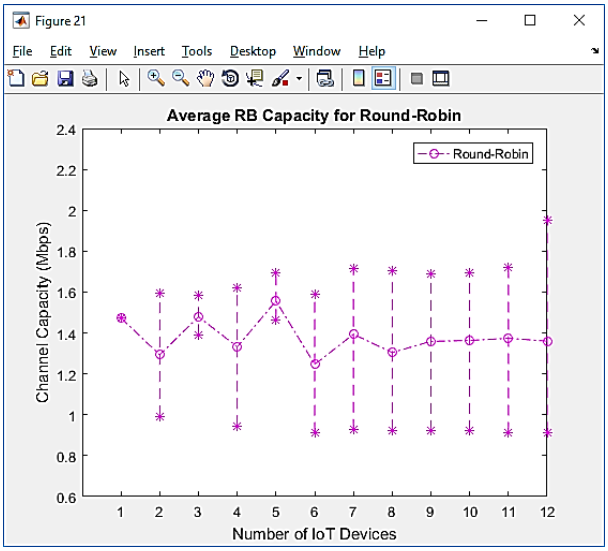

Figure 8d. Max, Min, and Average Capacity for Round-Robin

Table III: VALUES FOR MAX, MIN, AND AVERAGE RB CAPACITY OF ROUND ROBIN

# of Devices	RR (Max)	RR (Min)	RR (Avg)
1	1.4729	1.4729	1.4729
2	1.5935	0.9928	1.2932
3	1.5816	1.3895	1.4793
4	1.6214	0.9451	1.3318
5	1.6952	1.4648	1.5562
6	1.5891	0.9114	1.2464
7	1.7135	0.9266	1.3936
8	1.7025	0.9231	1.3043
9	1.6886	0.9207	1.3591
10	1.6951	0.9206	1.3633
11	1.719	0.912	1.374
12	1.9513	0.9138	1.3598

Table IV: VALUES FOR MAX, MIN, AND AVERAGE RB CAPACITY OF OEA

# of Devices	OEA (Max)	OEA (Min)	OEA (Avg)
1	1.9469	1.9469	1.9469
2	2.1304	1.944	2.0372
3	1.9123	1.6087	1.7415
4	2.2566	1.8001	2.0246
5	2.0406	1.5535	1.8189
6	2.1993	1.4667	1.8887
7	2.1705	1.6063	1.8892
8	2.2806	1.4099	1.9511
9	2.2974	1.0486	1.8293
10	2.2858	0.9287	1.7352
11	2.2173	0.8733	1.7643
12	2.2163	0.6213	1.621

Table V: VALUES FOR MAX, MIN, AND AVERAGE RB CAPACITY OF ENHANCED OEA

# of Devices	Enhanced OEA (Max)	Enhanced OEA (Min)	Enhanced OEA (Avg)
1	1.6177	1.6177	1.6177
2	1.77	1.6412	1.7056
3	1.6236	1.4099	1.5026
4	1.76	1.5011	1.613
5	1.6498	1.4217	1.5375
6	1.7902	1.1974	1.5549
7	1.7809	1.4598	1.6051
8	1.847	1.4388	1.6336
9	1.8476	1.31	1.526
10	1.7884	1.1898	1.4592
11	1.824	1.3595	1.4334
12	1.7785	1.1583	1.3131

To further examine the RB capacity behavior, the maximum, minimum, and average RB capacities were outputted as shown in Figure 8a-8d. The values of the results can be found in *Table III, Table IV,* and Table V. One of the notable differences between all three algorithms is the gap between the maximum and minimum RB capacity. Figure 9 shows a side-by-side comparison of the RB capacity for the OEA and proposed algorithms. Though the average RB capacity for OEA algorithm is greater than the average RB capacity for both the proposed and round-robin algorithms, the difference between the max and min grow as there are more IoT devices as seen in Figure 10 and Table VI. This is most likely due to the fairness in which RBs are allocated to IoT devices. The OEA is a greedy algorithm that pairs using the best raw metric. This means that RBs that are later allocated would likely have a lower SNR and this can be seen with the large difference in RB capacity as there are more IoT devices. The proposed algorithm takes the highest average SNR, leaving a more even distribution of RBs that have an adequate SNR. This is seen by looking at the difference between the maximum and minimum RB capacities.

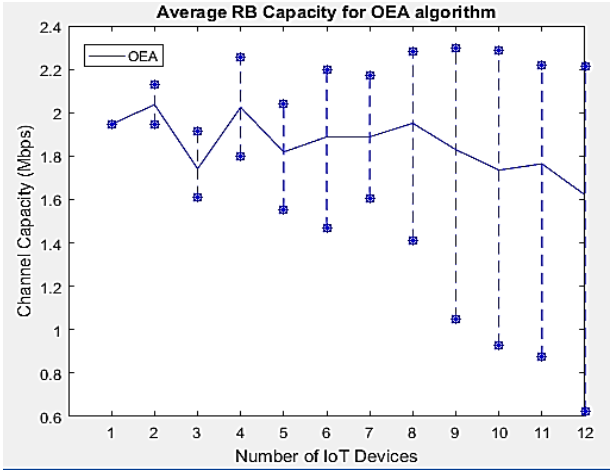

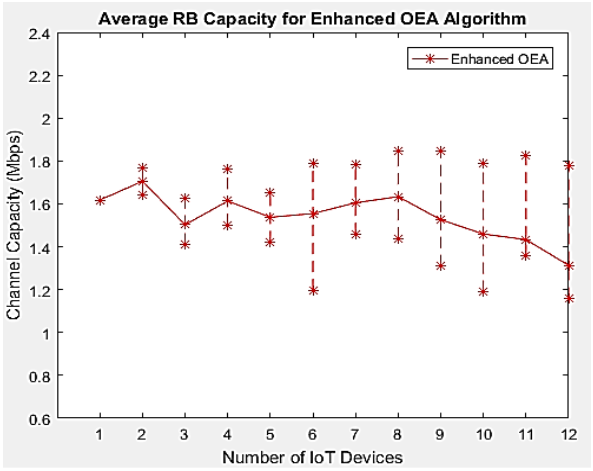

Figure 9. Comparison of Max, Min., and Avg. RB Capacity

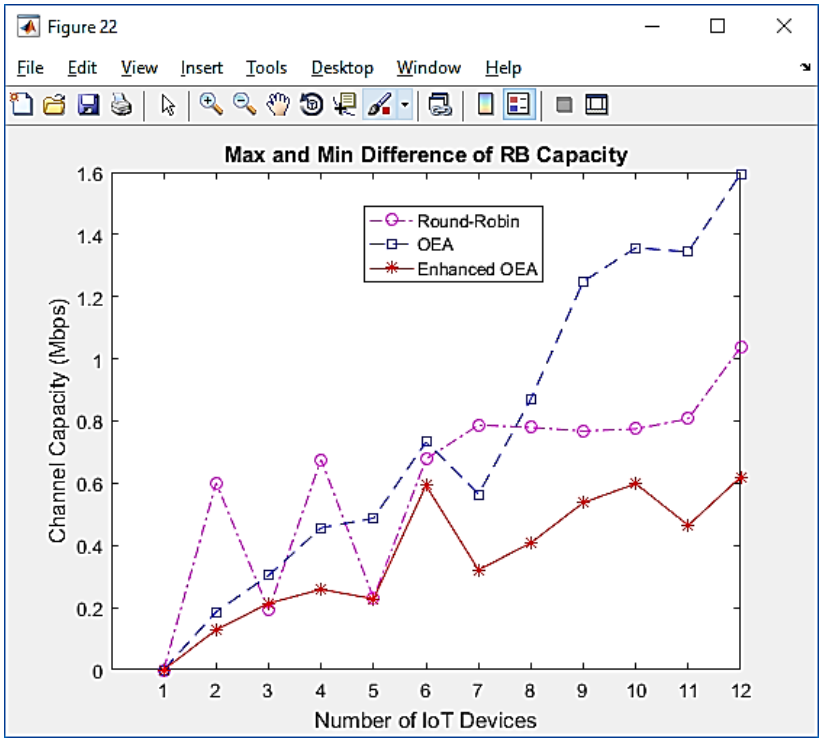

Figure 10. Max and Min Difference of RB Capacity

Table VI: VALUE FOR MAX AND MIN DIFFERENCE OF RB CAPACITY

# of Devices	Round Robin	OEA	Enhanced OEA
1	0	0	0
2	0.6007	0.1864	0.1288
3	0.1921	0.3035	0.2138
4	0.6763	0.4566	0.2588
5	0.2305	0.4871	0.2281
6	0.6777	0.7325	0.5929
7	0.7869	0.5642	0.3211
8	0.7795	0.8707	0.4083
9	0.7679	1.2488	0.5376
10	0.7746	1.3571	0.5987
11	0.8071	1.344	0.4645
12	1.0376	1.595	0.6201

iii.RB Utilization Ratio

RB utilization ratio can be defined as the total throughput divided by the total RB capacity. The overall throughput in the proposed algorithm is slightly higher than OEA algorithm, yet the RB capacity is lower.

However, the throughput is still consistently below the RB capacity and thus a higher percentage of the RB capacity is being used for the throughput. This results in a better RB utilization ratio as shown in Figure11 and Table XII below. The round-robin algorithm has a higher RB utilization ratio than the OEA algorithm because its RB capacity is generally less than OEA's resulting RB capacity.

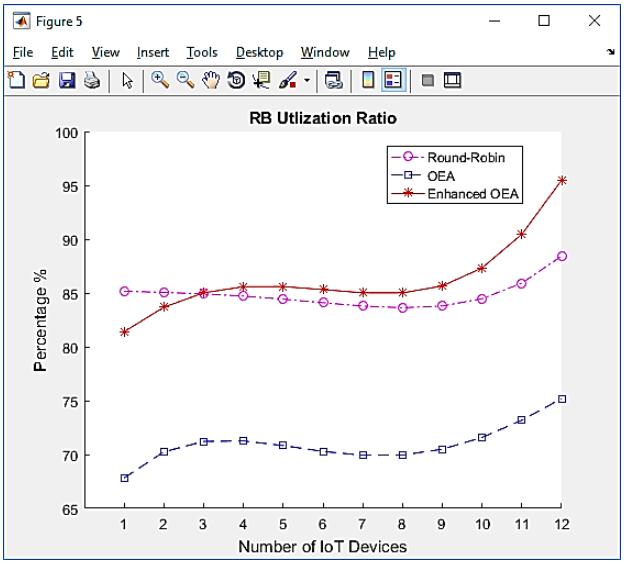

Figure 11. RB Utilization Ratio

Table VII: VALUES FOR RB UTILIZATION RATIO

# of Devices	Round Robin	OEA	Enhanced OEA
1	85.1688	67.8261	81.4038
2	85.0516	70.2504	83.6822
3	84.9175	71.2182	85.0137
4	84.7125	71.2606	85.5803
5	84.4264	70.8276	85.5973
6	84.0924	70.2876	85.3137
7	83.7872	69.928	85.012
8	83.6312	69.9547	85.0085
9	83.7884	70.4923	85.6529
10	84.4661	71.584	87.3285
11	85.9156	73.1919	90.4522
12	88.4314	75.1964	95.4744

The round-robin algorithm has a higher RB utilization ratio than the OEA algorithm because its RB capacity is generally less than OEA's RB capacity.

iv.Power Consumption

Initially, all IoT devices are assumed to use the maximum allowed power, which is 125 mW or 21 dBm. This is used to do the initial SNR calculation. After RB allocation has taken place, power control occurs and, if applicable, decreases the transmission power in order to attain the minimum required SNR, maintaining adequate channel for data transfer. The results of the power consumption are shown in Figure 12 and Table XIII below.

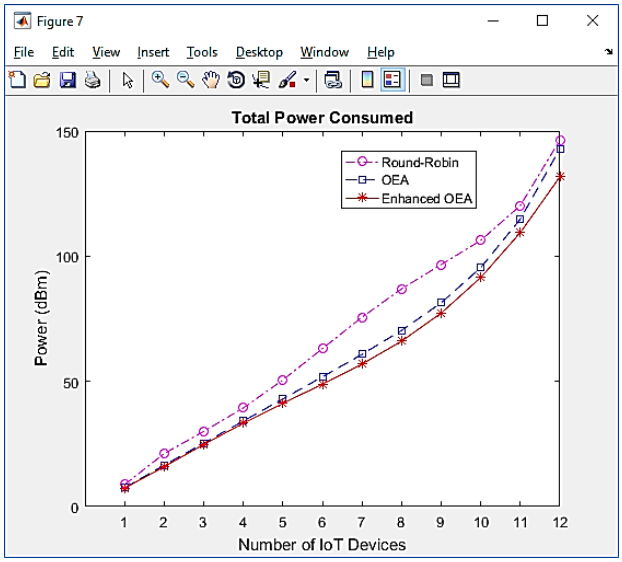

Figure 12. Total Power Consumed

Table VIII: VALUES FOR TOTAL POWER CONSUMED

# of Devices	Round Robin	OEA	Enhanced OEA
1	8.764	7.5002	7.3381
2	21.1379	16.5099	15.8976
3	30.0057	25.3242	24.7748
4	39.3722	34.1416	33.2656
5	50.5529	42.9748	41.2116
6	63.086	51.8137	48.8892
7	75.6426	60.7901	56.8991
8	86.9383	70.3407	66.0555
9	96.6442	81.371	77.2751
10	106.2978	95.4195	91.4667
11	120.2143	114.8208	109.4202
12	146.3975	142.8698	131.696

As there are more IoT devices, the proposed algorithm consumes less power than the OEA algorithm. The round-robin continually consumes a greater amount of energy than the other two algorithms. The proposed algorithm starts to consume less energy around the same place where the difference between the maximum and minimum RB capacity begin to differ from OEA algorithm, which is around 7 and 8 IoT devices. The average power consumed per device behaves consistently with the total power consumed. This can be examined in Figure 13 and Table XIV below. It is seen that at 11 devices the Round-Robin algorithm's average power consumption per device is close to the OEA algorithm. This is likely due to the fact that RBs that have a high SNR were allocated by chance and the RBs with lowest SNR were not allocated. This happens since allocation starts from the first index and simply allocates in order of index in the Round-Robin algorithm. Additionally, the number of RBs allocated are closer to the max number of RBs in the systems. Due to this, there is a higher chance that if the RBs with lower SNR were not allocated, then the power consumption of the Round-Robin would become similar to the OEA algorithm. Still, the power consumption in Round-Robin is generally greater than the OEA and Enhanced OEA algorithms.

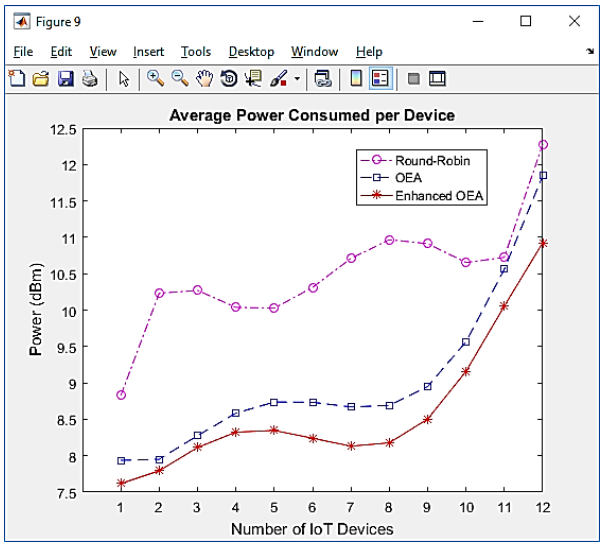

Figure 13. Average Power Consumed per Device

Table IX: VALUES FOR AVERAGE POWER CONSUMED PER DEVICE

# of Devices	Round Robin	OEA	Enhanced OEA
1	8.8283	7.9366	7.6175
2	10.2312	7.9511	7.793
3	10.2705	8.2757	8.1135
4	10.0375	8.5846	8.3232
5	10.0274	8.7373	8.3472
6	10.3118	8.7339	8.2397

7	10.7109	8.6697	8.1314
8	10.9663	8.6914	8.1771
9	10.9131	8.9516	8.504
10	10.6527	9.5648	9.1587
11	10.7249	10.5622	10.0559
12	12.2807	11.8471	10.9253

The average power consumed per device for the proposed algorithm is consistently lower than OEA algorithm, as well as the Round-robin algorithms. Consequently, the proposed algorithm saves more power as the number of IoT devices reaches the maximum number of devices that the eNodeB can serve. This is shown in Figure *14*14-15 and Table XV-XVI below.

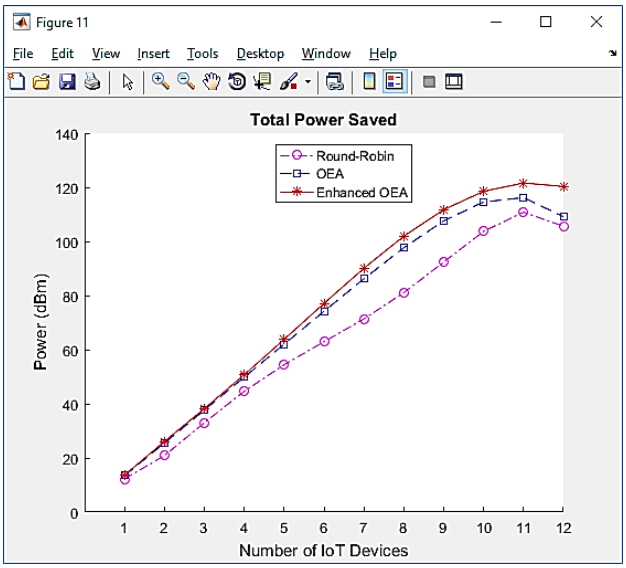

Figure 14. Total Power Saved

Table X: VALUES FOR TOTAL POWER SAVED

# of Devices	Round Robin	OEA	Enhanced OEA
1	12.236	13.4998	13.6619
2	20.8621	25.4901	26.1024
3	32.9943	37.6758	38.2252
4	44.6278	49.8584	50.7344
5	54.4471	62.0252	63.7884
6	62.914	74.1863	77.1108
7	71.3574	86.2099	90.1009
8	81.0617	97.6593	101.9445
9	92.3558	107.629	111.7249
10	103.7022	114.5805	118.5333
11	110.7857	116.1792	121.5798
12	105.6025	109.1302	120.304

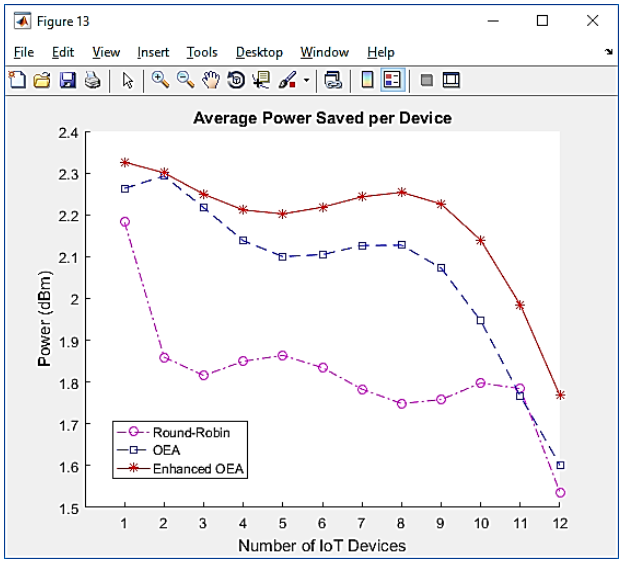

Figure 15. Average Power Saved per Device

Table XI: VALUES FOR AVERAGE POWER SAVED PER DEVICE

# of Devices	Round Robin	OEA	Enhanced OEA
1	2.1825	2.2631	2.3259
2	1.8595	2.293	2.3004
3	1.8156	2.2171	2.2492
4	1.8497	2.138	2.2115
5	1.8638	2.1	2.2023
6	1.8342	2.1049	2.2183
7	1.7829	2.1266	2.2432
8	1.7485	2.1273	2.2538
9	1.758	2.0725	2.2258
10	1.7976	1.9462	2.1392
11	1.7841	1.7666	1.9844
12	1.5363	1.6011	1.7677

v.Power Efficiency

Finally, the proposed algorithm increases the power efficiency when compared to the OEA algorithm as shown in Figure 15 and Table XVII. The power efficiency is calculated by taking the total throughput and dividing it by the total power consumed. The round-robin proves to have bad power efficiency compared to the OEA algorithm despite having a higher RB utilization ratio since it blindly allocates RB to each IoT device.

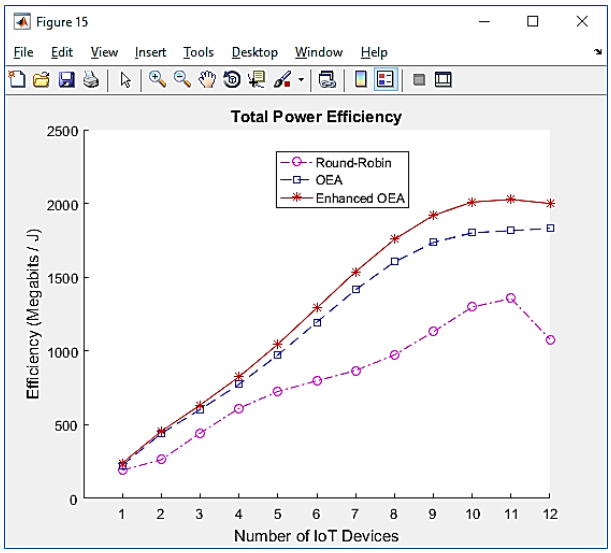

Figure 15. Total Power Efficiency

Table XII: VALUES FOR TOTAL POWER EFFICIENCY

# of Devices	Round Robin 1.0e+03 *	OEA 1.0e+03 *	Enhanced OEA 1.0e+03 *
1	0.1918	0.2258	0.2405
2	0.2625	0.4405	0.4556
3	0.443	0.6034	0.6335
4	0.6112	0.7739	0.8245
5	0.7253	0.9732	1.046
6	0.7975	1.1948	1.2912
7	0.867	1.4149	1.5379
8	0.9735	1.6037	1.7566
9	1.1303	1.7359	1.9197
10	1.2976	1.8012	2.0094
11	1.3558	1.8155	2.0267
12	1.0787	1.8315	1.9998

VII. Conclusion and Future Work

This research paper proposes an algorithm that is a modification of the opportunistic algorithm proposed in [17]. Using the same motivation behind SC-FDMA, which is to have a lower PAPR, the greedy algorithm from [17] was modified with an extra step to use the average calculated SNR to perform resource allocation. The modification increases the computational complexity but showed that it decreases power consumption and increases power efficiency when the number of IoT devices gets closer to the maximum number of devices that the eNodeB can serve. Thus the benefits of the algorithm reveals itself as there are more devices. One of the reasons behind this phenomenon could be

attributed to the smaller difference between the max and min of RB capacity, which translates to a more consistent SNR spread among the IoT devices.

In this paper, resource allocation was done in one instance of time. To improve the simulation, one can simulate a continuous allocation over time in order to further assess the power consumption and energy efficiency of the modified algorithm. Doing so would add the timing synchronization and parallelism complexity that would occur in practical applications of resource allocation. Building on top of this, having the simulation transfer data over a wireless channel using hardware resources would help to validate the saving of power consumption for the IoT devices. It would also further require that the algorithm complexity to be run within the 1 ms sub frame requirement in wireless transmission.

References

[1] A. Grassi, G. Piro, G. Bacci and G. Boggia, "Uplink resource management in 5G: when a distributed and energy-efficient solution meets power and QoS constraints," *IEEE Transactions on Vehicular Technology,* vol. PP, no. 99, pp. 1-1, 2016.

[2] Qualcomm Technologies, "Leading the world to 5G," Qualcomm Technologies, Inc., February 2016. [Online]. Available: https://www.qualcomm.com/documents/qualcomm-5g-vision-presentation. [Accessed 4 May 2017].

[3] Y. Li, Z. Yang and W. Xu, "Resource and power allocation for Uplink LTE networks with load and power coupling," in *8th International Conference on Wireless Communications & Signal Processing*, 2016.

[4] M. Viswanathan, "Log Distance Path Loss or Log Normal Shadowing Model," 30 September 2013. [Online]. Available: http://www.gaussianwaves.com/2013/09/log-distance-path-loss-or-log-normal-shadowing-model/. [Accessed 1 May 2017].

[5] A. Taufique, "LTE Power Control (Case of Uplink Channel: PUSCH," Tech Trained, LLC, June 2016. [Online]. Available: http://www.techtrained.com/lte-power-control/. [Accessed 4 May 2017].

[6] F. Ghavimi, Y.-W. Lu and H.-H. Chen, "Uplink Scheduling and Power Allocation for M2M Communications in SC-FDMA based LTE-A Networks with QoS Guarantees," *IEEE Transactions ,* vol. XX, no. YY, p. PP, 2016.

[7] Anritsu, "LTE Resource Guide," Anritsu Company, October 2009. [Online]. Available: http://web.cecs.pdx.edu/~fli/class/LTE_Reource_Guide.pdf. [Accessed 4 May 2017].

[8] I. C. Wong, O. Oteri and W. McCoy, "Optimal Resource Allocation in Uplink SC-FDMA Systems," *IEEE Transactions on Wireless Communications,* vol. 8, no. 5, pp. 2161-2165, 2009.

[9] Keysight Technologies, "LTE Physical Layer Overview," Keysight Technologies, 2016. [Online]. Available: http://rfmw.em.keysight.com/wireless/helpfiles/89600b/webhelp/subsystems/lte/content/lte_overview.htm. [Accessed 14 March 2017].

[10] M. A. N. Shukur, D. K. Pahwa and E. A. Singhal, "Implementing SC-FDMA & OFDMA in MATLAB," *International Journal of Computing and Corporate Research,* vol. 3, no. 6, 2013.

[11] B. Hanta, "SC-FDMA and LTE Uplink Physical Layer Design," University of Erlangen-Nüremberg (FAU), Erlangen, Germany, 2009.

[12] H. G. Myung, J. Lim and D. J. Goodman, "Single Carrier FDMA for Uplink Wireless Transmission," *IEEE Vehicular Technology Society,* vol. 1, no. 3, pp. 30 - 38, 2006.

[13] X. Zhang, X. S. Shen and L.-L. Xie, "Uplink Achievable Rate and Power Allocation in Cooperative LTE-Advanced Networks," *IEEE Transactions on Vehicular Technology,* vol. 65, no. 4, pp. 2196-2207, 2016.

[14] R. L. C. d. Reis and L. H. M. K. Costa, "4G - LTE/LTE-A OFDMA and SC-FDMA: Coursework for Computer Networks II," February 2014. [Online]. Available: https://www.gta.ufrj.br/ensino/eel879/trabalhos_vf_2014_2/rafaelreis/ofdma_scfdma.html. [Accessed 3 May 2017].

[15] K. C.-J. Lin, "Wireless Networking - Fundamentals and Applications Class," Academia Sinica: Research Center for IT Innovation, Taipei, 2010.

[16] I. Poole, "Comparison of 8-QAM, 16-QAM, 32-QAM, 64-QAM 128-QAM, 256-QAM, Types," Adrio Communications Ltd, November 2016. [Online]. Available: http://www.radio-electronics.com/info/rf-technology-design/quadrature-amplitude-modulation-qam/8qam-16qam-32qam-64qam-128qam-256qam.php. [Accessed 1 May 2017].

[17] F. Z. Kaddour, E. Vivier, M. Pischella and P. Martins, "Green Opportunistic and Efficient Resource Block Allocation Algorithm for LTE Uplink Networks," *IEEE Transactions on Vehicular Technology,* vol. 64, no. 10, pp. 4537-4550, 2015.

[18] A. Aijaz, M. R. Nakhai and A. H. Aghvami, "Power efficient uplink resource allocation in LTE networks under delay QoS constraints," in *IEEE Global Communications Conference*, Austin, TX, USA, 2014.

[19] A. Biral, H. Huang, A. Zanella and M. Zorzi, "Uplink Resource Allocation in Cellular Systems: An Energy-Efficiency Perspective," in *IEEE Global Communications Conference*, San Diego, CA, USA, 2015.

[20] M. Jar and G. Fettweis, "Throughput maximization for LTE uplink via resource allocation," in *International Symposium on Wireless Communication Systems (ISWCS)*, 28-31 Aug. 2012.

[21] I. Poole, "LTE UE Category & Class Definitions," Adrio Communications Ltd., November 2016. [Online]. Available: http://www.radio-electronics.com/info/cellulartelecomms/lte-long-term-evolution/ue-category-categories-classes.php. [Accessed 1 May 2017].

[22] LTE University, "How to calculate peak data rate in LTE," 18 February 2010. [Online]. Available: http://lteuniversity.com/get_trained/expert_opinion1/b/hongyanlei/archive/2010/02/18/how-to-calculate-peak-data-rate-in-lte.aspx. [Accessed 4 May 2017].

[23] A. Anisimov, "How to calculate LTE throughput," Nokia Siemens Networks, February 2016. [Online]. Available: http://anisimoff.org/eng/lte_throughput.html. [Accessed 4 May 2017].

[24] I. Poole, "Free Space Path Loss: Details, Formula, Calculator," Adrio Communications Ltd, [Online]. Available: http://www.radio-electronics.com/info/propagation/path-loss/free-space-formula-equation.php. [Accessed 14 March 2017].

[25] Wikipedia contributors, "Johnson-Nyquist noise," Wikipedia, 26 April 2017. [Online]. Available: https://en.wikipedia.org/wiki/Johnson%E2%80%93Nyquist_noise. [Accessed 4 May 2017].